

# TRACKLET-TRACKLET CORRELATION METHOD FOR RADAR AND ANGLE OBSERVATIONS

A. Vananti<sup>(1)</sup>, T. Schildknecht<sup>(1)</sup>, J. Siminski<sup>(2)</sup>, B. Jilete<sup>(3)</sup>, T. Flohrer<sup>(2)</sup>

<sup>(1)</sup> *Astronomical Institute, University of Bern, Sidlerstrasse 5, 3012 Bern, Switzerland, Email:*

*[alessandro.vananti@aiub.unibe.ch](mailto:alessandro.vananti@aiub.unibe.ch), [thomas.schildknecht@aiub.unibe.ch](mailto:thomas.schildknecht@aiub.unibe.ch)*

<sup>(2)</sup> *ESA/ESOC, Robert-Bosch-Strasse 5, 64293 Darmstadt, Germany, Email: [jan.siminski@esa.int](mailto:jan.siminski@esa.int), [tim.flohrer@esa.int](mailto:tim.flohrer@esa.int)*

<sup>(3)</sup> *ESA/ESAC, Villanueva de la Cañada, 28692, Madrid, Spain, Email: [beatriz.jilete@esa.int](mailto:beatriz.jilete@esa.int)*

## ABSTRACT

In the context of Space Surveillance and Tracking the observations provided by a network of sensors are processed and used to maintain a catalogue of orbital elements. The build-up of a catalogue and its maintenance depend on the capacity to determine the orbit of the observed objects from few measurements sparsely distributed on relative long arcs. The sparse observations or short sequences of observations need to be correlated or associated with each other. The association consists in identifying the series of observations, so-called tracklets, that belong to the same space object.

A method is proposed to associate radar tracklets, consisting of radar observations, to other radar tracklets or to optical tracklets acquired with optical sensors and consisting of angles-only observations. The association method is applied to different simulated observation scenarios and the performance of the algorithm is evaluated.

## 1 INTRODUCTION

In the context of Space Surveillance and Tracking the observations provided by a network of sensors are processed and used to maintain a catalogue of orbital elements. The build-up of a catalogue and its maintenance depend on the capacity to determine the orbit of the observed objects from few measurements sparsely distributed on relative long arcs. The sparse observations or short sequences of observations (tracklets) need to be correlated or associated with each other.

Recent work in this area can be found in the literature [1][2][3]. The developed methods until now are mainly related to observations from optical sensors. Recently some research group has started to investigate the association problem with observations containing ranges and range rates [4].

In this paper a method is proposed to associate radar tracklets (range and angle measurements) with each other and radar tracklets with optical tracklets (angle measurements from an optical sensor, telescope).

In the typical association problem all the tracklets observed during one or several nights are collected

together and all the possible combinations of two tracklets are evaluated according to a certain criterion. The existing methods differ in the way the tracklet is described, e.g. by attributables [1], and in the criterion used to evaluate whether an association is good or not, e.g. based on the Mahalanobis distance between parameters characterizing the two tracklets [2].

The observed tracklet in the radar case can be quite long depending on the Field of Regard (FoR) and the strategy adopted. In the strategy proposed by Mendijur et al. [5], for example, the considered FoR is 20° in elevation and 120° in azimuth. Note that in reality the arc length of the orbit covered by the radar observations is much less than the angles covered in the FoR, especially in the case of low orbits. Nevertheless for relative long tracklets covering several degrees of orbital arc and two or more observations the single tracklet might contain already enough information for a successful initial orbit determination.

If the initial orbit is available for both tracklets, the association of the two orbits can be evaluated comparing e.g. orbital parameters. For the association between a radar and an optical tracklet, only the orbit calculated from the radar measurements should be used. In fact optical tracklets, due to the limited field of view of the sensor and the chosen observation strategy, usually cover a shorter arc and it is difficult with these to compute an initial orbit. If for the optical tracklet a description with attributables is adopted, the orbit of the radar tracklet has then to be compared with the attributable of the second tracklet.

Hence the following basic scheme is proposed:

- Calculation of initial orbit from radar tracklet
- Propagation of orbit to epoch of second tracklet
- Comparison of propagated orbit with optical attributable or orbit calculated from second radar tracklet
- Computation of the associated orbit

In the following section these steps are explained in more details.

## 2 CORRELATION STEPS

### 2.1 Initial orbit determination

Two methods are considered to compute the initial orbit:

- The Lambert method [7], using two observations with angles and ranges, and the time difference between them.
- The “Range and Angles method” described in the Goddard Trajectory Determination System (GTDS) document [6], able to use more than two observations with an iteration scheme.

The GTDS Range and Angles method provides in most of the tested cases a more accurate initial orbit determination than the Lambert method, probably because it can use all the observations of the tracklet. Only the tracklets with a configured minimum number of observations are selected for the orbit determination process. The obtained initial orbit has still to be refined with a least squares approach where ranges and angles are weighted differently. At this stage, for some tracklets the least squares will fail to converge, while for other tracklets the root mean square (rms) calculated in the least squares fitting exceeds a configured threshold and are discarded.

### 2.2 Propagation

The orbit calculated from the radar tracklet has to be propagated to the epoch of the second tracklet. Also the covariance in the orbital elements, obtained after the least squares procedure for the radar tracklet, is propagated to the epoch of the second tracklet. Here the transition matrix from the first to the second epoch has to be calculated. The covariance is necessary for the comparison with the second tracklet. The propagation is performed in analytical or numerical way:

- Analytical propagation, needs shorter computation time, but does not consider perturbations.
- Numerical propagation, perturbations are taken into account, but the iterative procedure is in general slower.

In the proposed approach the numerical propagation is used when the inclusion of perturbations is important in the association process, especially if the tracklets are separated by more than one revolution, or the tracked object is at low altitude and is more influenced by gravity perturbations. For this part of the processing the model implemented in the Orekit library [8] is adopted. Earth’s gravity terms up to degree and order 4, air drag, solar radiation pressure, and luni-solar forces are considered. The transition matrix is calculated with a finite difference scheme and is used for the propagation of the covariance.

### 2.3 Association of radar orbits

Similarly to the case with optical tracklets, the comparison of radar orbits can be done using the definition of Mahalanobis distance [2] as a measure of the goodness of the association. The limitation with this measure is in the description of the uncertainty distribution, modeled according to the covariance in a Gaussian distribution. Mostly the Gaussian assumption is enough to describe the uncertainty in the orbital parameters, but depending on the coordinate system the inadequacy can be accentuated. For example, in a Cartesian system is difficult to describe the typical “banana” shaped elongation of the error ellipsoid, due to the faster increase in the along-track uncertainty. Several methods have been developed to take into account non-Gaussian distributions in propagation and tracklet association [9][10]. Sometimes an appropriate coordinate system can be found where the Gaussian assumption approximates the actual distribution. The along-track elongation, for example, can be better described in spherical coordinates than in Cartesian coordinates.

The Mahalanobis distance  $L$  is given by

$$L = (P_1 - P_2)^T \cdot (C_1 + C_2)^{-1} \cdot (P_1 - P_2)$$

where  $P_1, P_2$  are vectors, in a certain coordinate system, representing the first and second orbit, while  $C_1, C_2$  are their covariance matrices. The use of the above definition for the goodness of an association can be justified in mathematical terms with probabilistic considerations related to the multivariate Gauss distribution [2]. It can be shown that the distribution of Mahalanobis distances, with a Gaussian uncertainty in the vectors, follows a  $\chi^2$  distribution with  $k$  degrees of freedom, where  $k$  depends on the tracklet association method. Based on this property a threshold can be defined below which the association is accepted with a certain confidence level.

In the proposed approach the Mahalanobis distance is calculated in two different coordinate systems:

- Cartesian coordinates, difficult description of the uncertainty distribution
- Curvilinear coordinates [11], more suitable to describe the orbital uncertainty distribution

Curvilinear coordinates are an improvement of the known transformation to the Hill frame, where the position of a moving object (e.g. target), relative to the coordinate system centered at another moving object (e.g. interceptor), is given. Essentially the transformation to curvilinear coordinates takes into account the real curved trajectory of the target. As a consequence in this coordinates system the expected “banana” shaped ellipsoid is not curved any longer and the uncertainty can be better approximated with a Gaussian distribution.

## 2.4 Association of radar orbit with optical attributable

In the association of radar orbits with optical attributables the radar orbit is propagated to the second epoch as in the radar-radar association case. However, the comparison is evaluated against an attributable that only contains angular positions and rates, i.e. only four parameters instead of the six orbital parameters. Thus, the propagated positions and velocities are transformed into the state in spherical coordinates but only the angular components are considered (without the radial position and rate) in the Mahalanobis distance. The covariance w.r.t. position and velocity has also to be transformed into the new basis with angular components.

## 2.5 Computation of the associated orbit

After the best tracklet association is found, the final orbit using the complete set of observations in the two associated tracklets is computed. Here a least squares improvement of the available radar initial orbit is performed. Different weights for radar and optical measurements may be adopted in the weight matrix. The rms obtained in the least squares fitting, and weighted according to the average measurement errors, is taken into account to still discard, defining a maximal value, the wrong tracklet associations.

## 3 SIMULATIONS AND RESULTS

First results were obtained with simulated radar and optical measurements. For the association of radar tracklets three scenarios are chosen with LEO objects on almost circular orbits (eccentricity  $< 0.01$ ) at different altitudes, around 400 km, 800 km, and 1000 km. For these three regions the ranges in semimajor axis cover:

- 7300 km  $< a <$  7500 km
- 7100 km  $< a <$  7300 km
- 6400 km  $< a <$  7000 km

The objects from the Space-Track TLE catalogue are observed during one night from a station at 40° latitude. Table 1 shows the values used for the simulation.

In the association of radar with optical tracklets a scenario considering a GTO population is selected, with perigee height 0-2000 km, apogee height 25000-40000 km, and inclination  $< 20^\circ$ . For the radar observations the same values in Table 1 apply, but a radar pointing at 90° azimuth and 70° elevation from a station at 0° latitude was chosen for better visibility conditions. The settings for the optical observations are indicated in Table 2. Furthermore constraints in the observed altitude are set to ensure that the objects are observed at perigee by the radar and at apogee by the optical sensor.

Radar pointing	Az. 180°, El. 60°
FoR	Az. 120°, El. 20°
Error ( $\sigma$ ) in range	5 m
Error ( $\sigma$ ) in angle	15'
Interval betw. obs.	10 s

Table 1. Values for the simulated radar observations for radar tracklets association.

Optical pointing	RA 20°, DEC 0°
FoR (fence)	RA 2°, DEC 30°
Error ( $\sigma$ ) in angle	1''
Interval betw. obs.	20 s

Table 2. Values for the simulation of optical observations.

The tracklet association procedure with the above described scheme was applied in the different scenarios. The initial orbit was calculated with the GTDS method, propagated with a Keplerian model, and for the radar tracklets association, the Mahalanobis distance was computed in curvilinear coordinates. In the initial orbit determination only tracklets with at least 3 observations were considered. A threshold of 10 in the Mahalanobis distance and a threshold of 5 for the maximal acceptable rms in the least squares calculation of initial and final associated orbit were chosen.

A summary of the results is given in Table 3. The rows have the following meaning:

- number of tracklets: the total number of tracklets considered
- excluded: indicates the number of tracklets excluded because the number of observations in the tracklet is below the configured minimum of 3.
- failed IOD: indicates the number of radar tracklets excluded because the initial orbit determination failed. This happens when the least squares fit does not converge or the obtained rms exceeds the configured threshold of 5
- correl.: the number of correlations (ground truth)
- excl. correl.: the number of correlations excluded due to an excluded tracklet
- fail. correl.: the number of correlations excluded due to tracklets where the IOD failed
- net correl.: the remaining number of correlations after subtracting the excluded and failed correlations
- number of correct correlations (true positives)
- number of false positives

	LEO 400km	LEO 800km	LEO 1000km	GTO
number of tracklets	775	3821	1024	344
excluded	183	508	118	24
failed IOD	7	56	25	99
correl.	154	1267	264	40
excl. correl.	80	284	56	0
fail. correl.	3	37	15	11
net correl.	71	946	193	29
true pos.	34	382	125	17
false pos.	122	409	16	0

Table 3. Summary of the results for the different scenarios.

### 3.1 LEO correlation

In the correlation of LEO objects at least half of the simulated correlations remain after excluding too short and “failed IOD” tracklets. Most of the exclusions are due to short tracklets, while the failed IOD concerns only less than 5% of the correlations. This reflects the situation of the total tracklets number and excluded tracklets, although the percentage of “failed IOD” tracklets is even lower. In the actual correlation step, starting from the net number of correlations, the true positives vary from 40% to 65% depending on the scenario altitude. It is expected a major difficulty in the correlation at lower altitudes. In fact the dwell time, shown in Figure 1, Figure 2, and Figure 3, decreases with the altitude and a consequence could be a reduced accuracy in the initial orbit determination.

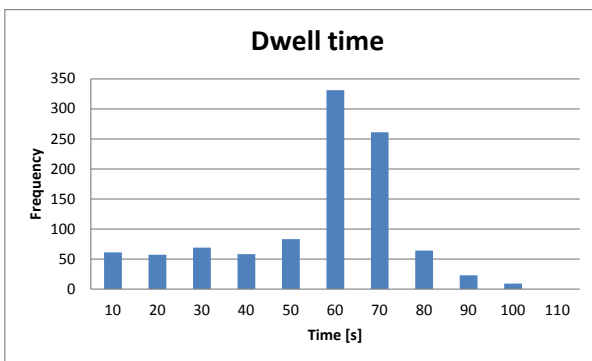


Figure 1: Dwell time of the objects at around 1000 km altitude.

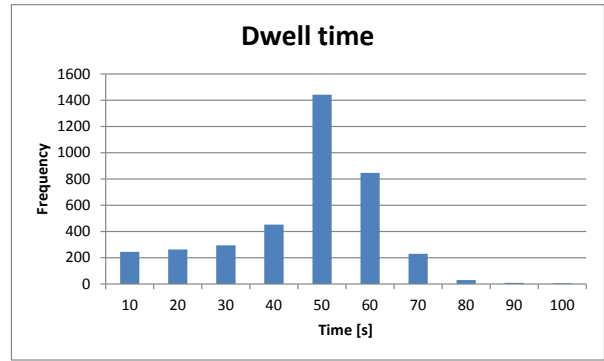


Figure 2: Dwell time of the objects at around 800 km altitude.

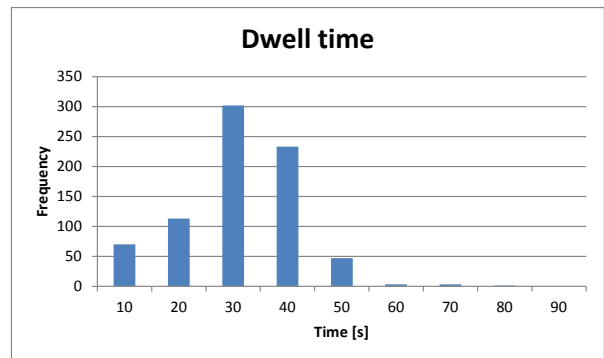


Figure 3: Dwell time of the objects at around 400 km altitude.

The distribution of Mahalanobis distances, taking into account both true and false positives, is shown in Figure 4, Figure 5, and Figure 6, for the three different scenarios. The number of false positives at 1000 km is quite low, around 1/10 of the true positives. The histogram shows a clear asymptotic trend to smaller values at higher Mahalanobis distances. The population of objects strongly increases in the 800 km scenario. As a consequence the number of false positives is much bigger and even exceeds the one of true positives. The histogram in Figure 5 reaches a plateau at higher Mahalanobis distances. The choice of the threshold is in general dictated by a compromise in terms of correct correlations and rejected false alarms. The relative number of false positives is even larger in the 400 km scenario. Although the population is not so dense in this region a lower accuracy, as mentioned above, is probably responsible for the major number of false alarms.

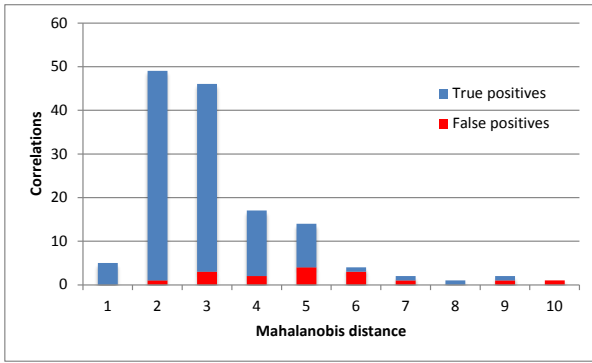


Figure 4: Mahalanobis distance distribution for true and false positives in the scenario at 1000 km.

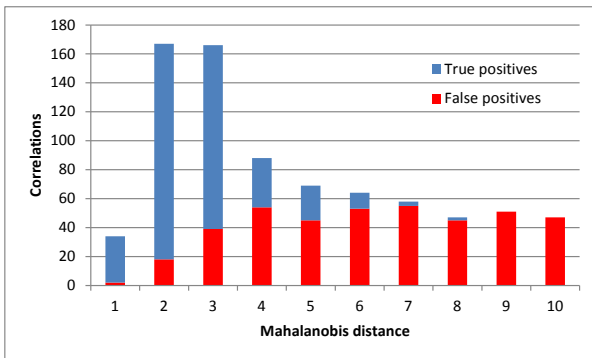


Figure 5: Mahalanobis distance distribution for true and false positives in the scenario at 800 km.

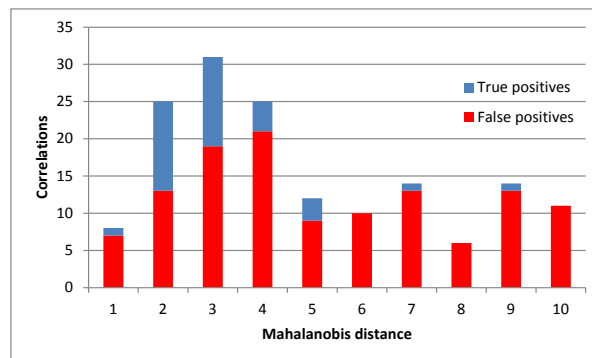


Figure 6: Mahalanobis distance distribution for true and false positives in the scenario at 400 km.

As previously explained in the correlation procedure, there are two types of threshold for the selection of the valid tracklet associations. One threshold is based on the Mahalanobis distance, while the second, applied at the end, takes into account the rms obtained in the least squares procedure to calculate the final orbit. To show the influence of the rms threshold, an example with a scenario similar to the one at 400 km with a reduced population and no false positives is considered. The distribution of the rms keeping the threshold for the Mahalanobis distance at 10, is shown in Figure 7. This

indicates that an rms threshold of 5 eliminates a big amount of false positives. Figure 8 shows the Mahalanobis distribution for an rms of 1000, which essentially represents the case without any rms threshold. Note that many false positives are still present with a Mahalanobis distance smaller than 10. These can be reduced thanks to the rms threshold limitation as illustrated in Figure 9, where a threshold of 200 is chosen. Then with the usual rms threshold of 5, in this scenario all false positives are eliminated.

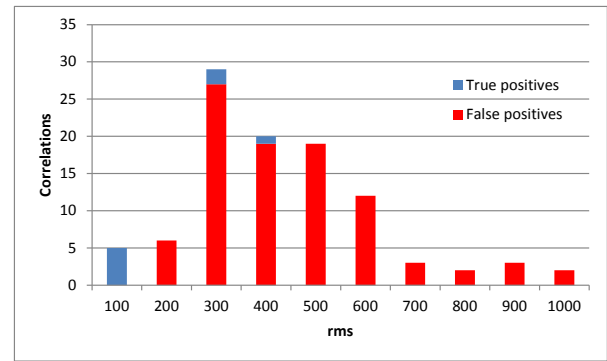


Figure 7: Rms distribution of true and false positives for example scenario at 400 km.

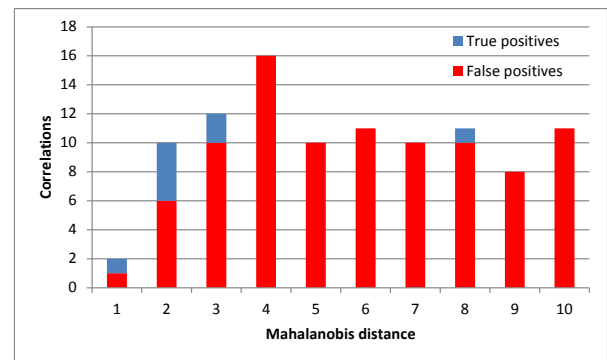


Figure 8: Mahalanobis distance distribution with rms threshold of 1000 in the example scenario at 400 km.

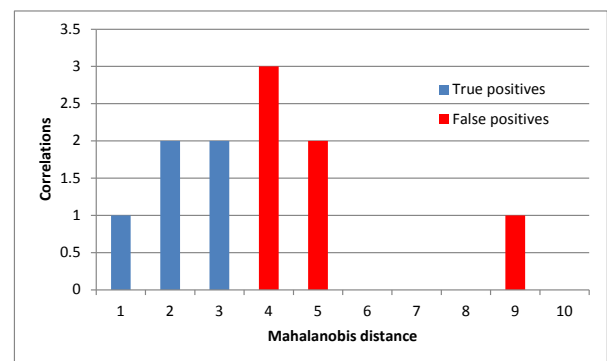


Figure 9: Mahalanobis distance distribution with rms threshold of 200 in the example scenario at 400 km.

### 3.2 GTO Correlation

In this scenario contrary to the LEO case, the reason for the reduced number of net correlations is mostly the failed IOD. This suggests a major difficulty in the initial orbit determination due probably to the high eccentric GTO orbit.

The range of dwell time for radar FoR and optical fence is characterized by the choice of the object population constrained at apogee and perigee. Most of the objects have a radar dwell time lower than 100 s, closer to the interval observed in the pure LEO scenario. Different dwell times in the optical fence reflect the population with a broad range of apogee altitudes.

More than half of the net number of associations is found, with no false positives. The distribution of the Mahalanobis distances is shown in Figure 12.

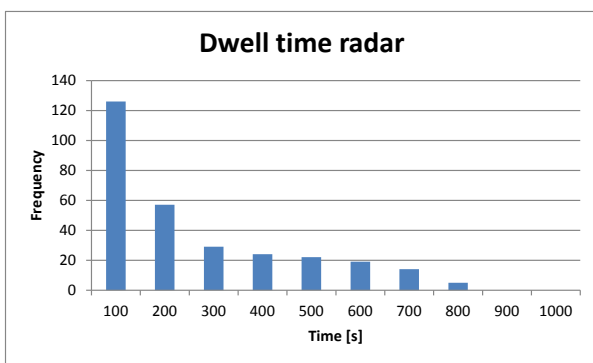


Figure 10: Dwell time of the GTO objects in the radar FoR.

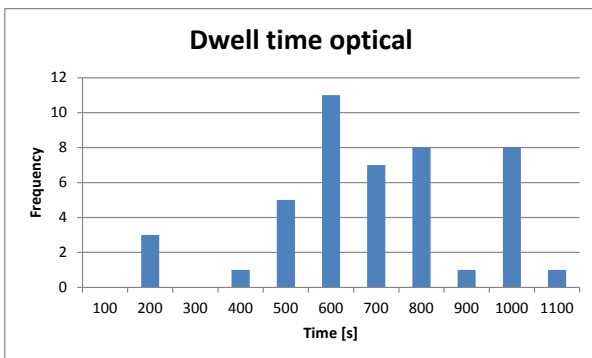


Figure 11: Dwell time of the GTO objects in the optical fence.

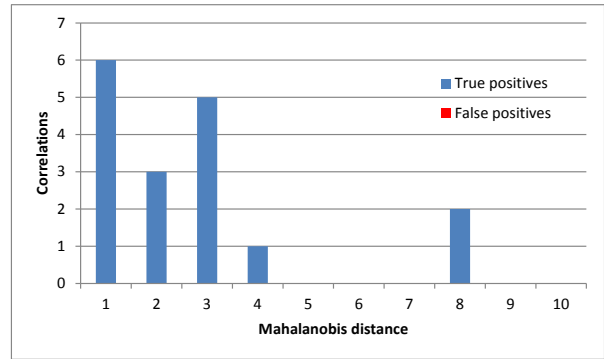


Figure 12: Mahalanobis distance distribution for true positives in the GTO scenario.

## 4 CONCLUSIONS

A method to associate radar tracklets on one hand and optical with radar tracklets on the other hand is proposed. The method consists in different steps including: the initial orbit determination from a single radar tracklet, the propagation to the epoch of the second tracklet, the comparison of the propagated orbit with an optical attributable or an orbit calculated from the second radar tracklet, and the computation of the associated orbit. In the comparison with orbit or attributable the Mahalanobis distance is used to evaluate the goodness of the tracklet association. An appropriate coordinate system is chosen, in which the orbit uncertainty is better described. For the comparison of two orbits computed from radar tracklets, the choice of a system of curvilinear coordinates give good results. If the second tracklet consists of optical measurements, spherical coordinates are considered. A threshold in the Mahalanobis distance is the first selection criterion to accept a considered association. The second criterion sets a limit on the rms in the least squares orbit improvement computed with two associated orbits. Three scenarios in LEO with different altitudes were simulated. The number of correct associations, after excluding too short tracklets, ranges from 40% to 60%, while the amount of false alarms varies with the selected altitude and is influenced by the density of the object population and the length of the observed arc. For the association of radar and optical tracklets a scenario with GTO objects was proposed. Here more than half of the correct associations was found and no false alarm. In this scenario a major difficulty in the initial orbit determination is observed, probably caused by a higher eccentricity of the considered orbits. The results show that the developed approach is able to find a reasonable number of correct associations in the LEO and GTO regimes. Further scenarios have to be evaluated with different algorithm options and different threshold values to better characterize the capabilities of the proposed method.

## 5 ACKNOWLEDGEMENTS

This activity was conducted under ESA's SSA Programme (project 4000112524/14/D/MRP).

## 6 REFERENCES

1. Milani, A., Tommei, G., Farnocchia, D., Rossi, A., Schildknecht, T., Jehn, R. (2012). Correlation and orbit determination of space objects based on sparse optical data. *Monthly Notices of the Royal Astronomical Society* **417**.
2. Siminski, J., Montenbruck, O., Fiedler, H., Schildknecht, T. (2014). Short-arc tracklet association for geostationary objects. *Advances in Space Research* **53**.
3. Fujimoto, K., Scheeres, D.J., Herzog, J., Schildknecht, T. (2014). Association of optical tracklets from a geosynchronous belt survey via the direct Bayesian admissible region approach. *Advances in Space Research* **53**.
4. Gronchi, G.F., Farnocchia, D., Dimare, L. (2011). Orbit determination with the two-body integrals (II). *Celestial Mechanics and Dynamical Astronomy* **110**.
5. Mendijur, M., Sciotti, M., Besso, P. (2012). Management of radar resources for space debris tracking. *Proceedings of SPIE* **8385**.
6. Long, A.C., Cappellari, J.O., Velez, C.E., Fuchs, A.J. (1989). *Goddard Trajectory Determination System (GTDS)*. Computer Sciences Corporation & National Aeronautics and Space Administration / Goddard Space Flight Center, Greenbelt, MD.
7. Izzo, D. (2015). Revisiting Lambert's problem. *Celestial Mechanics and Dynamical Astronomy* **121**.
8. *Orekit (Orbits Extrapolation KIT)*, a space dynamics library in Java, [www.orekit.org](http://www.orekit.org)
9. Hussein, I., Demars, K., Frueh, C. (2012). An AEGIS-FISST Algorithm for Multiple Object Tracking in Space Situational Awareness. *Proceedings of AIAA/AAS Astrodynamics Specialist Conference*, Minneapolis, MN.
10. Horwood, J.T., Poore, A.B., Alfriend, K.T. (2011). Orbit determination and data fusion in GEO. *Proceedings of 12<sup>th</sup> AMOS Conference*, Maui, Hawaii.
11. Vallado, D., Alfano, S. (2014). Curvilinear coordinate transformations for relative motion. *Celestial Mechanics and Dynamical Astronomy* **118**.